

1 **Lipid-encapsulated mRNAs encoding complex fusion proteins potentiate anti-tumor immune**
2 **responses**

3 Casey W. Shuptrine¹, Yuhui Chen¹, Jayalakshmi Miriyala¹, Karen Lenz¹, Danielle Moffett¹, Thuy-Ai Nguyen¹, Jenn
4 Michaux¹, Kristen Campbell¹, Connor Smith¹, Marc Morra¹, Yisel Rivera-Molina¹, Noah Murr¹, Sarah Cooper¹,
5 Ashlyn McGuire¹, Vishruti Makani¹, Nathan Oien¹, Jeffery T. Zugates¹, Suresh de Silva¹, Taylor H. Schreiber¹,
6 Seymour de Picciotto² and George Fromm¹

7 ¹Shattuck Labs Inc., Austin TX and Durham NC

8 ²Moderna, Inc., Cambridge MA

9 **Running Title:** mRNA-encoded fusion proteins induce anti-tumor immunity

10 Corresponding Author: George Fromm, 21 Alexandria Way, Suite 200, Durham, NC 27709
11 (919) 864-2700, gfromm@shattucklabs.com

12 **Abstract (249 words)**

13 Lipid nanoparticle (LNP)-encapsulated mRNA has been used for *in vivo* production of several secreted
14 protein classes, such as IgG, and has enabled the development of personalized vaccines in oncology.
15 Establishing the feasibility of delivering complex multi-specific modalities that require higher-order
16 structures important for their function could help expand the use of mRNA/LNP biologic formulations.
17 Here, we evaluated whether *in vivo* administration of mRNA/LNP formulations of SIRP α -Fc-CD40L and
18 TIGIT-Fc-LIGHT could achieve oligomerization and extend exposure, on-target activity, and anti-tumor
19 responses comparable to that of the corresponding recombinant fusion proteins. Intravenous infusion of
20 the formulated LNP-encapsulated mRNAs led to rapid and sustained production of functional hexameric
21 proteins *in vivo*, which increased the overall exposure relative to the recombinant protein controls by
22 ~28-140 fold over 96 hours. High concentrations of the mRNA-encoded proteins were also observed in
23 secondary lymphoid organs and within implanted tumors, with protein concentrations in tumors up to
24 134-fold greater than with the recombinant protein controls 24 hours after treatment. In addition,
25 SIRP α -Fc-CD40L and TIGIT-Fc-LIGHT mRNAs induced a greater increase in antigen-specific CD8⁺ T cells in
26 the tumors. These mRNA/LNP formulations were well tolerated and led to a rapid increase in serum and
27 intratumoral IL-2, delayed tumor growth, extended survival, and outperformed the activities of
28 benchmark monoclonal antibody controls. Furthermore, the mRNA/LNPs demonstrated improved
29 efficacy in combination with anti-PD-L1 relative to the recombinant fusion proteins. These data support
30 the delivery of complex oligomeric biologics as mRNA/LNP formulations, where high therapeutic
31 expression and exposure could translate into improved patient outcomes.

32 **Statement of Significance:** Lipid nanoparticle-encapsulated mRNA can efficiently encode complex fusion
33 proteins encompassing immune checkpoint blockers and co-stimulators that functionally oligomerize *in*
34 *vivo* with extended pharmacokinetics and durable exposure to induce potent anti-tumor immunity.

35 **Conflict of Interest Disclosure Statement:** Casey Shuptrine, Yuhui Chen, Jayalakshmi Miriyala, Karen Lenz, Jenn
36 Michaux, Danielle Moffett, Kristen Campbell, Connor Smith, Marc Morra, Thuy-Ai Nguyen, Yisel Rivera-Molina,
37 Noah Murr, Sarah Cooper, Ashlyn McGuire, Vishruti Makani, Nathan Oien, Jeffery T. Zugates, Suresh de Silva,
38 Taylor Schreiber, and George Fromm are employees and shareholders of Shattuck Labs, Inc.. Seymour de Picciotto
39 is an employee and shareholder of Moderna, Inc..

40

41 Introduction

42 At the core of the successful global response to the SARS-CoV-2 pandemic lies decades of research
43 dedicated to the synthesis of mRNAs incorporating unique sequence elements and modifications. These
44 modifications enhance their stability and translation efficiency. To enable their effective delivery, lipid
45 nanoparticles (LNPs) have been developed to encapsulate the mRNA cargo, providing protection and
46 facilitating transport into the cytosol of target cells (1,2). mRNA/LNP technology has been applied to a
47 wide variety of protein formats, including the expression of a full-length neutralizing antibody to
48 Chikungunya virus (3-6). Application of mRNA/LNP technology to antibodies requires the separate
49 expression and pairing of both immunoglobulin heavy and light chains into the appropriate quaternary
50 structure for secretion, stability and function *in vivo*. Other advances have enabled the development of
51 personalized vaccines in oncology, including mRNA-4157, wherein patient-specific tumor antigens are
52 rapidly identified and assembled as concatemers into a continuous mRNA capable of stimulating anti-
53 tumor immune responses. In patients with high-risk melanoma, mRNA-4157 in combination with
54 pembrolizumab, resulted in recurrence free survival at 18 months in 78.6% of patients, compared to
55 62.2% of patients with pembrolizumab alone (7,8). Current efforts aimed at enhancing the systemic
56 safety of mRNA/LNP formulations, and reducing immunogenicity risks following repeated
57 administration, are beginning to show promise in clinical studies, and may open the door for broader
58 proliferation of mRNA/LNP formulations of biologics as an economical alternative to mass-produced
59 recombinant proteins (9). Thus, establishing feasibility for the expression and assembly of complex
60 biologics when delivered as mRNA/LNP formulations, and comparing the biologic properties of *in vivo*
61 expressed biologics to bolus-injected recombinant proteins, are important goals.

62 SIRP α -Fc-CD40L and TIGIT-Fc-LIGHT are two such biologics that have been developed as recombinant Fc-
63 fusion proteins in humans and non-human primates, respectively (Figure 1A)(10-12). Each of these
64 recombinant proteins are expressed from single continuous open reading frames (ORFs) by CHO cells.
65 Following the expression of a protein monomer, covalent dimers form through interchain disulfide
66 bonds in the Fc region of the protein. Dimers then assemble first into tetramers and ultimately
67 hexamers due to non-covalent trimerization by the TNF ligand domains (10,11,13,14)(Figure 1B-C). This
68 oligomerization is crucial for the activity of TNF-ligands and their cognate TNF receptors (like CD40, 4-
69 1BB, OX40, and others), which require trimerization in the cell membrane to effectively signal and
70 induce immune cell agonism (Figure 1D)(14-16).

71 The goals of the current study were to determine the efficiency of expression of SIRP α -Fc-CD40L and
72 TIGIT-Fc-LIGHT as mRNA/LNP formulations, assess whether the mRNA-encoded proteins attained
73 functional hexameric structures *in vivo*, and to compare the biological activity of the mRNA/LNP
74 expressed constructs to the corresponding recombinant fusion protein reference material (Figure 1B)(FP
75 ref.). We found that intravenous infusion of mRNA/LNPs was well tolerated, and concentrations of the
76 mRNA-encoded protein exceeded that of the FP ref. protein within two hours of delivery in serum and
77 other tissues. The primary structure of the mRNA-encoded protein in the serum of treated animals *in*
78 *vivo* was confirmed to be a hexamer, as the high serum concentrations facilitated purification and SEC
79 analysis of the oligomer composition. To further confirm the potency of hexameric SIRP α -Fc-CD40L and
80 TIGIT-Fc-LIGHT as lipid encapsulated mRNAs, the pharmacodynamic and anti-tumor activity of these
81 formulations was compared to the well characterized recombinant protein equivalents using a large
82 established CT26 colorectal carcinoma tumor model. In total, these studies confirmed that lipid-

83 encapsulated mRNA encoding *SIRP α -Fc-CD40L* and *TIGIT-Fc-LIGHT* dramatically extended the *in vivo*
84 exposure of predominantly hexameric fusion proteins, with improved pharmacodynamic and anti-tumor
85 effects when compared head-to-head against the corresponding recombinant protein. Taken together,
86 these results support the evaluation of complex secreted biologics by mRNA/LNP delivery.

87

88 **Materials and Methods**

89 *Material Generation and Characterization*

90 The generation of FP ref. material was accomplished as previously described, through transient
91 production in CHO cells followed by affinity capture of the mouse constructs using protein A and human
92 constructs using FcXL, followed by elution and buffer exchange(10,11). mRNA constructs were
93 synthesized by *in vitro* transcription (IVT) followed by DNase digestion. A plasmid encoding the T7 RNA
94 polymerase promoter followed by 5'untranslated region (UTR), open reading frame (ORF), 3'UTR, and
95 polyA tail was overexpressed in *E. coli*, linearized, and purified to homogeneity. The mRNA was
96 synthesized by using a modified T7 RNA polymerase IVT, where uridine triphosphate was substituted
97 completely with N1-methyl-pseudouridine triphosphate. Cap 1 was utilized to improve translation
98 efficiency(17). After the transcription reaction, mRNAs were purified, buffer exchanged into sodium
99 citrate, and stored at -20 °C until use. Formulation of mRNA were performed as described
100 previously(18). Analytical characterization assays included particle size and polydispersity,
101 encapsulation, and endotoxin content which had to meet predefined specifications before the material
102 was deemed acceptable for *in vivo* study. The mRNA was encapsulated in a lipid nanoparticle through a
103 modified ethanol-drop nanoprecipitation process described previously (18). Briefly, ionizable, structural,
104 helper, and PEG lipids were mixed with mRNA in acetate buffer, pH 5.0, at a ratio of 3:1 (lipids:mRNA).
105 The mixture was neutralized with Tris-Cl, pH 7.5, sucrose was added as a cryoprotectant, and the final
106 solution was sterile filtered. Vials were filled with formulated LNP and stored frozen at -70 °C until
107 further use. The final drug product underwent analytical characterization, which included the
108 determination of particle size and polydispersity, encapsulation, mRNA purity, and endotoxin. Final
109 particle size and encapsulation were <100 nm and >80%, respectively, with endotoxin below 10 EU/mL.
110 Both FP ref. material and protein encoded by mRNA contain a wild-type mouse IgG1 central domain.

111 *In vitro Functional Activity*

112 *HEK293 Transfection:* 1 μ g of naked mRNA with Lipo2000 was used to transfect HEK293T cells
113 (RRID:CVCL_0063). After 24 or 48 hours, cell culture supernatant was collected, and mouse and human
114 mRNA-encoded proteins were purified as described above. SDS-PAGE was used to characterize the
115 purified FP using antibodies targeting mouse and human SIRP α , CD40L, TIGIT, LIGHT, or Fc (R&D Systems
116 and The Jackson Laboratory). mRNA-encoded FP were quantitated using MSD (Meso Scale Discovery) as
117 described using the corresponding recombinant FP control as a standard(12).

118 *MSD Potency:* Dual target binding MSD assays were developed for each construct to ensure full-length
119 protein was capable of engaging its intended targets at the same time, as previously described(10,11).
120 Here, FP ref. and mRNA-encoded proteins were assessed using capture/detect reagents to mouse and
121 human CD47/CD40 or PVR/HVEM.

122 *Cell-Based Potency Assays:* CHOK1-CD40/NFκB-luciferase cells were previously generated (10) and used
123 to assess luciferase dose responses of FP ref. and mRNA-encoded material. Macrophage/tumor
124 phagocytosis assays were performed as previously described(10). RAW264.7-Lucia-ISG-reporter cells
125 (InvivoGen, RRID:CVCL_X596) were used according to manufacturer recommendations to assess CD40
126 activation of a type I interferon stimulatory reporter in the presence of mouse SIRPα-Fc-CD40L FP ref. or
127 the mRNA-encoded material. PathHunter U2OS/LTβR/NIK/NFκB reporter cells (DiscoverX) were used
128 according to manufacturer recommendations to assess the activity of TIGIT-Fc-LIGHT FP ref. and mRNA
129 material. LTβR+ A375 (RRID:CVCL_0132) or CT26 (RRID:CVCL_7254) tumor cell lines were cultured with
130 test agents for 3 hours before reverse transcribing cDNA to assess the expression of ACTB, CXCL8, CCL2,
131 and CXCL5 using qPCR with SYBR green reagents, validated primer sequences from Origene, and the Bio-
132 Rad CFX96 Touch real-time PCR detection system. Fold change in gene expression was determined using
133 the ΔΔCt method relative to the housekeeping gene ACTB (11).

134 Reporter cell lines were obtained from the indicated vendors. Parental cell lines were purchased from
135 ATCC. Cells in active culture were passaged 2-3 times per week, kept in culture for a maximum of two
136 months, and tested monthly using the Venor GeM Mycoplasma Detection Kit (Sigma). All transfected
137 cell lines were tested an additional two times post transfection, separated by at least 2 weeks, and
138 confirmed to remain negative for mycoplasma.

139 *In vivo PK, PD, and anti-Tumor Activity*

140 *Pharmacokinetics:* BALB/c (8-12 week old female, The Jackson Laboratory, RRID:MGI:2161072) mice
141 were given a single intravenous tail vein injection of vehicle (PBS), mRNA/LNP constructs (0.5 mg/kg or
142 12.5 μg in total), or FP reference material (8 mg/kg or 200 μg in total); 3 mice per group per time point.
143 Tissues and serum were isolated and cell lysates were prepared at the indicated timepoints to
144 determine FP concentrations using a MSD-dual binding assay, and normalized as pg or ng per gram of
145 starting tissue. For SEC, serum samples were diluted with PBS and loaded onto an AKTA Start protein
146 purification system at a flow rate of 0.11 mL/min, using a 1 mL HiTrap column and Amsphere A3 protein
147 A resin. Eluted material was assessed by SEC using a Thermo Fisher Scientific Vanquish system with a Bio
148 SEC-5 (Agilent, 500Å, 5μm, 7.8 ID x 300 m).

149 *Pharmacodynamics:* Serum chemistries were evaluated by the Pathology Service Core and Animal
150 Clinical Laboratory Medicine Core at the University of North Carolina at Chapel Hill, using the Vet Axcel
151 Chemistry Analyzer (Alfa Wassermann). Serum and tumor lysate cytokines were assessed using a custom
152 MSD multiplex plate according to manufacturer instructions. Resulting data was plotted in heatmap
153 format depicting row min/max values across samples. Hierarchical clustering (1- Spearman correlation)
154 was used to demonstrate group and cytokine associations.

155 *Tumor Efficacy:* BALB/c mice (8 to 12 weeks old) were subcutaneously implanted with 5×10^5 CT26 tumor
156 cells into the hind right flank. When tumors were approximately 90 mm³ (8 days after inoculation on
157 average) mice were randomized across treatment groups and treatment was initiated (indicating day 0).
158 Tumor-bearing mice were treated via intraperitoneal (IP) injections with recombinant fusion proteins
159 (200 μg per dose) and antibodies (100 μg per dose for anti-CD47 (clone MIAP410 BioXCell,
160 RRID:AB_2687806) and anti-TIGIT (clone 1G9 BioXCell, RRID:AB_2687797) or 200 μg per dose for anti-
161 PDL1 (clone 10F.9G2, RRID:AB_10949073) or via IV injection for the mRNA/LNP constructs (0.5 mg/kg
162 per dose) on Days 0, 3, 7, 10, 14, and 17 of a 30-day time course. The anti-tumor efficacy benchmark for

163 these fusion protein constructs and antibodies has previously been described using IP administration,
164 and we and others have shown that IP and IV administration in mice results in similar drug exposure
165 levels (Supplemental Figure 1A)(10,11,19). Tumor volume (mm³) and overall survival were assessed
166 throughout the time-course. Animals were humanely euthanized when total tumor volume reached
167 >1800 mm³ or there were signs of significant tumor ulceration. Individual animal tumor growth curves,
168 the average time in which each treatment group reached full tumor burden, the number of mice that
169 rejected the primary tumor (tumor volume ≤0.5 mm³), and overall survival were assessed over a 30-day
170 time-course. On Day 8 of the study, a group of treated animals was euthanized, and necropsy was
171 performed to collect serum and tumor tissue for PK, cytokine, and flow cytometry analysis.

172 *Flow Cytometry:* Tumor tissue was dissociated using an enzymatic tumor dissociation kit (Miltenyi
173 Biotec), and the resulting cells were exposed to a viability dye and then Fc receptors were blocked (both
174 BioLegend). Cell staining was performed for 30 minutes at 4°C in the dark. For FoxP3 staining, the FoxP3
175 fix/perm buffer kit (BioLegend) was used according to manufacturer instructions. After antibody
176 incubations, cells were washed 2x in 500 µL FACS buffer (1x DPBS, 1%BSA, 2 mM EDTA, and 0.02%
177 NaN₃), and then analyzed on the BD LSR Fortessa Cell Analyzer.

178 *Experimental Animal Guidelines*

179 All experimental mice used were female inbred BALB/c co-housed during the course of an experiment
180 (The Jackson Laboratory). All murine animal studies have been conducted in accordance with, and with
181 the approval of an Institutional Animal Care and Use Committee (IACUC); and reviewed and approved by
182 a licensed veterinarian.

183 *Statistical Analysis*

184 Unless noted otherwise, values plotted represent the mean and error is SEM. Statistical significance (p-
185 value) was determined using One-Way ANOVA with multiple comparisons. Significant p-values are
186 labeled with one or more ‘*’, denoting *p<.05, **p<.01, ***p<.001 and ****p<.0001. Mantel-Cox
187 statistical tests were used to determine the significance between the survival curves.
188

189 *Data Availability*

190 Data were generated by the authors and included in the article. All raw data are available upon request
191 from the corresponding author.

192

193 **Results**

194 mRNA encoding mouse and human *SIRPα-Fc-CD40L* and *TIGIT-Fc-LIGHT* were transiently transfected
195 into HEK293T cells and after 24 or 48 hours, supernatant was collected and affinity purified. The
196 resulting protein was assessed using SDS-PAGE and were detected with three separate domain-specific
197 antibodies. All three detection methods indicated full length proteins migrating at the expected
198 monomeric molecular weights of 88.1 kDa for *SIRPα-Fc-CD40L* and 59.3 kDa for *TIGIT-Fc-LIGHT* (Figure
199 2A-B and Supplemental Figure 1B-C)(10,11). Secreted protein concentrations were evaluated using a
200 dual-binding MSD method, normalized on a per-cell-basis and found to reach 7.76 pg/cell at 24 hours
201 and 27.4 pg/cell at 48 hours for human *SIRPα-Fc-CD40L*, and 4.46 pg/cell at 24 hours and 8.98 pg/cell at

202 48 hours for human *TIGIT-Fc-LIGHT*; which are on par with the productivity achieved from commercial
203 CHO and 293 based biomanufacturing processes (Figure 2C-D) (20). Parallel studies using the mouse-
204 equivalent mRNA constructs showed similar results (Supplemental Figure 1D-E).

205 The potency of the mRNA-encoded proteins was assessed using (1) dual-target MSD potency, (2) cell-
206 based CD40/NFκB-luciferase reporter, and (3) *in vitro* species-specific macrophage phagocytosis assays
207 for *SIRPα-Fc-CD40L* (Figure 2C). Additionally, a RAW264.7/ISG (interferon stimulatory gene) reporter cell
208 line was used to inform on the activation of interferon response pathways downstream of CD40 ligation
209 (Supplemental Figure 1D, parts 1-4). Human mRNA-encoded *TIGIT-Fc-LIGHT* was assessed using (1) dual-
210 target MSD potency, (2) cell-based U2OS/LTβR/NFκB/Nik-luciferase reporter, and (3) through the
211 activation of CCL2 and CXCL8 expression in LTβR+ A375 tumor cells (Figure 2D). Mouse TIGIT-Fc-LIGHT
212 activity was assessed using a (1) dual-target MSD potency, and (2) through the activation of Ccl2 and
213 Cxcl5 expression in LTβR+ CT26 tumor cells (Figure 2D). The recombinant fusion protein material (FP
214 ref.) was used as a reference standard to calculate the concentration of the mRNA supernatants. In all
215 cases, the mRNA-encoded fusion proteins demonstrated equivalent potency to that of the FP ref.
216 material. Taken together, the *in vitro* results suggested that both *SIRPα-Fc-CD40L* and *TIGIT-Fc-LIGHT*
217 were efficiently produced from mRNA/LNPs and assembled into functional higher-order quaternary
218 structures capable of agonizing trimeric TNF receptors in various cell-based potency assays.

219 To determine whether expression and bioactivity was achievable *in vivo*, BALB/c mice were given a
220 single tail vein injection of 0.5 mg/kg (12.5 μg) of the LNP formulated mRNA or 8 mg/kg (200 μg) of the
221 FP ref. After 0.5, 1, 2, 6, 24, 48, 72, and 96 hours, serum, liver, spleen, and iLN were isolated from
222 treated animals for the analysis of serum chemistries and cytokines, and serum and tissue quantification
223 of mRNA encoded protein (Figure 3A). All test articles were well tolerated and no significant elevations
224 of ALT, AST, LDH, creatinine, or total bilirubin were observed over that of the vehicle treated group
225 (Supplemental Figure 1F). Dual MSD PK assays (capture with anti-mouse CD40L and detect with anti-
226 mouse SIRPα or capture with anti-mouse LIGHT and detect with anti-mouse TIGIT) were used to assess
227 serum concentrations of the fusion proteins delivered as recombinant protein or mRNA/LNP
228 formulations. As expected, the serum concentration for bolus injected recombinant SIRPα-Fc-CD40L and
229 TIGIT-Fc-LIGHT was highest at the first post-dose timepoint (0.5 hours) and decreased rapidly thereafter
230 (Figure 3B). The targets for SIRPα-Fc-CD40L (CD47 and CD40) are more abundant than the targets for
231 TIGIT-Fc-LIGHT (PVR, HVEM, LTβR), and accordingly both the C_{max} (maximum concentration) and AUC
232 (area under the curve) were higher for TIGIT-Fc-LIGHT as compared to SIRPα-Fc-CD40L (Figure 3B)(10-
233 12). Remarkably, serum *SIRPα-Fc-CD40L* and *TIGIT-Fc-LIGHT* were detectable at the earliest timepoint in
234 both mRNA/LNP treated groups, and the concentration of protein remained consistently high across the
235 entire time course. Further, the concentration of mRNA/LNP expressed proteins remained higher than
236 the C_{max} in the recombinant protein treated groups through 48 hours for *SIRPα-Fc-CD40L* and through
237 the entire 96-hour time course for *TIGIT-Fc-LIGHT*. The overall protein C_{max} from *SIRPα-Fc-CD40L* mRNA
238 treatment was 1.8-fold higher than the FP ref. and was not achieved until 12 hours post-dose, compared
239 to 0.5 hours for the FP ref. control. The AUC from *SIRPα-Fc-CD40L* mRNA was 140-fold greater than that
240 achieved with the FP ref. (Figure 3B). Similar kinetics were observed with *TIGIT-Fc-LIGHT* mRNA, with a
241 C_{max} 6.1-fold higher, and an AUC 28.7-fold greater than that seen with the FP ref. material. The
242 maximum serum concentration for *TIGIT-Fc-LIGHT* was not reached until 32 hours post-dose (t_{max})
243 compared to 0.5 hours for the FP ref.. In addition to achieving elevated concentrations in the serum,

244 both mRNA/LNP formulations also translated to higher concentrations with more sustained exposures in
245 the liver, spleen, and inguinal lymph nodes (Figure 3C).

246 To assess the oligomeric structure of the fusion proteins, we took advantage of the high serum
247 concentrations of mRNA-encoded fusion proteins which facilitated affinity purification of SIRP α -Fc-
248 CD40L directly from the serum of treated animals, followed by size exclusion chromatography (SEC).
249 When the absorbance spectrum from the mRNA/LNP serum sample was overlaid with a known and
250 well-characterized human SIRP α -Fc-CD40L reference standard, the serum isolated mRNA-encoded
251 material was found to closely share the oligomeric profile and existed primarily as a hexamer (Figure
252 3D).

253 The administration of both *SIRP α -Fc-CD40L* and *TIGIT-Fc-LIGHT* mRNA/LNPs led to significantly elevated
254 serum concentrations of IL-2, which persisted for 48-96 hours following a single dose (Figure 3E). With
255 the FP reference material, we have previously observed transient increases in IL-2 and other innate and
256 adaptive immune cytokines, including IL-2, MCP5, IP10, and MIP1 β , and observed similar results here
257 (Figure 3F)(10,11).

258 We next evaluated the pharmacodynamic and anti-tumor responses in mice bearing CT26 colorectal
259 tumors. Some mice were euthanized 24 hours post-dose and tumor tissue was dissociated and fusion
260 protein concentrations were assessed. In the *SIRP α -Fc-CD40L* group, 122-fold more protein was
261 detected in the tumors of mRNA/LNP treated animals compared to that of the FP ref. (220 pg/gram of
262 tissue vs. 1.8 pg/g). In the *TIGIT-Fc-LIGHT* group, 134.8-fold more protein was detected in the tumors of
263 mRNA/LNP treated animals compared to that of the FP ref. (13.48 ng/gram of tissue vs. 0.1 ng/g)(Figure
264 4A). The increased serum and tissue exposures (including in the tumor) mediated by the mRNA/LNP
265 delivery of *SIRP α -Fc-CD40L* and *TIGIT-Fc-LIGHT*, resulted in higher levels of serum and intra-tumor
266 expressed cytokines and chemokines (Figure 4B). In both the serum and tumor, unbiased hierarchical
267 clustering associated the SIRP α -Fc-CD40L and TIGIT-Fc-LIGHT treatment groups (both mRNA/LNP and FP
268 ref.) in proximity, suggesting that both therapeutic delivery methods achieved similar on-target
269 pharmacodynamic activity. In the tumor, the mRNA/LNP and FP ref. groups clustered a single branch
270 apart and appeared to differ by the overall magnitude of response, which was greater and broader in
271 the mRNA/LNP groups than what was observed with the FP reference material. Here, increased tumor
272 levels of IL2, IFN γ , IL-12p70, MDC, TNF α , MIP1 α , MIP1 β , MIP3 α , and MCP1, were observed in all
273 mRNA/LNP and FP ref. treatment groups compared to vehicle or benchmark checkpoint inhibitor
274 antibody reference controls (anti-CD47 or anti-TIGIT)(Figure 4B). These proinflammatory cytokines have
275 been associated with the activation of myeloid cells through both CD40 and LT β R(11,21). However,
276 interesting construct-dependent differences in the magnitude of cytokine expression were seen in the
277 serum and tumors of treated animals, including for MIP1 β , MCP1, MIP2, and MDC (Figure 3E-F, Figure
278 4B, and Supplemental Figure 1G)(10-12).

279 We next assessed whether mRNA/LNP formulations of *SIRP α -Fc-CD40L* or *TIGIT-Fc-LIGHT* could delay
280 the growth of established CT26 tumors and extend survival. Once tumors reached an average starting
281 tumor volume of $\sim 90\text{mm}^3$, mice were randomized and treated with either vehicle, anti-CD47, anti-TIGIT,
282 an irrelevant mRNA/LNP negative control, *SIRP α -Fc-CD40L* mRNA/LNP, SIRP α -Fc-CD40L FP ref., *TIGIT-Fc-*
283 *LIGHT* mRNA/LNP, or TIGIT-Fc-LIGHT FP ref. (Figure 4C). In the control groups, the average time it took
284 for mice to reach tumor burden was approximately 13-14 days following the first treatment. SIRP α -Fc-
285 CD40L FP ref. extended the time until reaching tumor burden to 18.80 days and the mRNA/LNP

286 extended this time to 23 days. The TIGIT-Fc-LIGHT FP ref. extended the time until reaching tumor
287 burden to 17.50 days and the mRNA/LNP extended this time to 23 days (Figure 4C). Several of the
288 treated mice completely rejected the established tumors, including with each of the mRNA/LNP groups.
289 The delay in tumor growth induced by the mRNA/LNP and FP ref. constructs also translated into
290 significant survival benefits over the vehicle control (Figure 4D).

291 Given the anti-tumor effects and observed changes in both serum and tumor cytokines and
292 chemokines, an analysis of tumor infiltrating lymphocytes was performed. Regulatory T cells (Treg;
293 CD4+CD25+Foxp3+) were not elevated in treatment groups, and instead the median percentage of Tregs
294 in the *TIGIT-Fc-LIGHT* mRNA group was 33.9% less than that of the vehicle control. All fusion protein and
295 mRNA treatments increased the infiltration of activated antigen-specific CD8+ T cells into the tumor
296 microenvironment (TME)(Figure 4E and Supplemental Figure 1H). *SIRP α -Fc-CD40L* and *TIGIT-Fc-LIGHT*
297 mRNAs induced the greatest increases in antigen-specific CD8+ T cells into the tumors (AH1 tetramer+),
298 with median values 1.62 and 2.29-fold greater than the vehicle group, respectively.

299 The efficacy of both *SIRP α -Fc-CD40L* and *TIGIT-Fc-LIGHT* were enhanced in combination with tumor
300 targeting antibodies that promote ADCC/ADCP and block checkpoint pathways(10,11). To further
301 characterize this combination activity with the mRNA-encoding constructs, anti-tumor activity and the
302 tumor infiltration of antigen-specific CD8+ T cells was evaluated in CT26 tumor bearing animals treated
303 with *SIRP α -Fc-CD40L* and *TIGIT-Fc-LIGHT* FP or mRNA/LNP in combination with anti-PDL1 (Figure 4F-G).
304 Consistent with previous findings, the combination of all constructs with anti-PDL1, significantly
305 improved tumor growth inhibition compared to anti-PDL1 on its own, with the mRNA/LNP combinations
306 demonstrating improved efficacy relative to the FP combinations (Figure 4G)(10,11). The mRNA/LNP +
307 anti-PDL1 combination groups also increased intratumoral percentages of CD8+CD69+ and CD8+AH1-
308 tetramer+ T cells compared to the corresponding monotherapy groups. *SIRP α -Fc-CD40L* mRNA + anti-
309 PDL1 increased CD8+CD69+ T cells 1.93-fold and CD8+AH1-tetramer+ T cells 2.75-fold greater than anti-
310 PDL1 monotherapy, and *TIGIT-Fc-LIGHT* mRNA + anti-PDL1 increased CD8+CD69+ T cells 1.72-fold and
311 CD8+AH1-tetramer+ T cells 2.33-fold greater than anti-PDL1 monotherapy (Figure 4G). These results
312 provide confirmation that *SIRP α -Fc-CD40L* and *TIGIT-Fc-LIGHT* mRNA encode functional fusion proteins
313 *in vivo*, which retain the pharmacodynamic and anti-tumor properties previously described for the
314 recombinant protein versions of these constructs.

315

316 Discussion

317 This study aimed to determine whether lipid encapsulated mRNA could be utilized to deliver complex Fc
318 fusion proteins that require self-association into hexamers through a mixture of covalent and non-
319 covalent interactions, via intravenous infusions. *SIRP α -Fc-CD40L* and *TIGIT-Fc-LIGHT* mRNA/LNP
320 formulations encoded functional fusion protein both *in vitro* and *in vivo*. The kinetics of both *SIRP α -Fc-*
321 *CD40L* and *TIGIT-Fc-LIGHT* detected concentrations through mRNA/LNP delivery was higher than that
322 achieved with a bolus delivery of recombinant fusion protein and was maintained across at least 96
323 hours. The progressive increase in expression of CD40L and LIGHT (contained within each fusion
324 protein), closely mirrors the native expression of these and other TNF ligands in the context of a
325 pathogen-induced immune response. In contrast, many TNF receptor agonist therapeutics that are
326 administered by intravenous infusion achieve maximal serum concentrations within a period of minutes

327 and then decay thereafter. Whether these distinct pharmacokinetic profiles contribute to distinct
328 differentiation states of the target cells for each TNF ligand is unknown at this time.

329 The primary site of *in vivo* protein production using intravenous administered mRNA/LNP is often shown
330 to be the liver, and consistently here, the highest concentrations of both SIRP α -Fc-CD40L and TIGIT-Fc-
331 LIGHT were detected in the serum and liver. Lower – but significant – amounts of both mRNA-encoded
332 proteins were detected in the spleen, lymph node, and within the tumor. The current study did not
333 differentiate between protein that was synthesized in a tissue versus proteins accumulated in that tissue
334 via diffusion or active transport from other compartments, however previous work has confirmed the
335 integration of mRNA within these tissues in similar studies ((6) and unpublished data). Regardless of the
336 mechanism, systemic exposure of both SIRP α -Fc-CD40L and TIGIT-Fc-LIGHT was increased when
337 administered as lipid encapsulated mRNA formulations.

338 The serum concentration of SIRP α -Fc-CD40L was high enough to enable the purification and SEC analysis
339 of the *in vivo* expressed protein, and remarkably, the prominent species was shown to exist as a
340 hexamer. When fusion proteins like SIRP α -Fc-CD40L or TIGIT-Fc-LIGHT are produced as recombinant
341 proteins from CHO cells, the final therapeutic exists primarily as a hexamer (10,11,22). The observation
342 here that intravenous infusion of mRNA/LNP results in hexameric TNF-ligand containing fusion proteins
343 *in vivo*, suggests that the necessary elements for oligomerization are present at the site of *in vivo*
344 translation. In future studies, it would be interesting to extend these observations to other routes of
345 administration, such as intramuscular and subcutaneous (23,24).

346 Previously published studies demonstrated anti-tumor activity for SIRP α -Fc-CD40L and TIGIT-Fc-LIGHT
347 fusion proteins in a range of preclinical models. Those data provided the pre-clinical basis to advance
348 SIRP α -Fc-CD40L (SL-172154) into clinical trials for patients with platinum resistant ovarian cancer, and
349 also patients with TP53 mutant AML and HR-MDS (NCT05483933 and NCT05275439, respectively),
350 where initial anti-tumor activity has been observed (10,11,25,26). Despite these data, a potential
351 limitation of this current study is that anti-tumor activity was only demonstrated in a single pre-clinical
352 mouse tumor model. Using the established CT26 tumor model, mRNA/LNP formulated SIRP α -Fc-CD40L
353 and TIGIT-Fc-LIGHT compared favorably to the recombinant protein counterparts. Treatment of mice
354 with large established tumors with SIRP α -Fc-CD40L or TIGIT-Fc-LIGHT recombinant protein extended
355 survival in comparison to groups treated with CD47 or TIGIT blocking antibodies. Survival was further
356 improved when the same fusion protein constructs were delivered as mRNA/LNPs, which is likely due to
357 increased exposure within the tumor, and because of prolonged pharmacodynamic effects compared to
358 the recombinant proteins. Delivery of SIRP α -Fc-CD40L as mRNA/LNP was associated with increased
359 tumor infiltration of antigen-specific CD8+ T cells, activated APCs, as well as high serum and tumor IL-2
360 levels that were distinct from other groups and persisted over the entire 96-hour time course. Whereas
361 the increase in IL-2 was consistent with *de novo* production, increases in many other serum cytokines
362 occurred within a few hours of treatment, and are likely due to the release of those cytokines and
363 chemokines from pre-formed granules in circulating immune cells, as has also been shown in human
364 cancer patients treated with SIRP α -Fc-CD40L(25,26). In other studies, elevation in chemokines like CCL3
365 and CCL20 were associated with infiltration of immunosuppressive myeloid and Th17 cells in the tumor
366 microenvironment(27). The current study was not focused on the assessment of these cell populations,
367 and future studies could aim to investigate this further.

368 One of the barriers to delivering biologics using lipid encapsulated mRNAs has been toxicity and
369 immunogenicity associated with the LNP component. Recent advances in LNP and mRNA optimization
370 have reduced these risks, and clinical studies currently underway in children with propionic acidemia
371 (NCT04159103) have demonstrated that mRNA-3957 was well tolerated for over a year of chronic
372 therapy (9). These findings are important as the use of lipid encapsulated nucleic acid technologies
373 continue to broaden into other disease areas that require chronic and sometimes lifelong treatment, for
374 example in various oncology indications or autoimmune disorders. The compelling expression of
375 complex biologics via mRNA/LNP formulations presented here, opens the door to exploring nucleic acid
376 delivery of other therapeutic scaffolds in broader populations of patients, previously thought to be
377 unreachable by an mRNA cargo. Recent studies have shown that lipid encapsulated mRNA can also be
378 used to facilitate *in vivo* production of functional monoclonal antibodies and T cell engagers, which do
379 not require oligomerization but instead require assembly of heavy and light chains independently
380 translated from distinct open reading frames(28-31). The speed, cost, and efficiency of mRNA/LNP
381 manufacturing, as well as improved expression, biodistribution, and pharmacodynamics, could result in
382 future approaches where biologics are developed and assessed in parallel with their RNA counterparts,
383 to provide optionality for the optimal targeting of particular receptors or ligands, based on desired PK
384 and PD characteristics that could be uniquely provided by the delivery of a biologic or an mRNA/LNP.
385 The studies herein demonstrate that such approaches may not be limited to individual cytokines,
386 antibodies, or enzymes, but could also apply to complex biologics such as SIRP α -Fc-CD40L and TIGIT-Fc-
387 LIGHT.

388

389 **Acknowledgements:** Funding to complete the work presented in this manuscript was provided by
390 Shattuck Labs, Inc. and Moderna, Inc.

391

- 393 1. Kiaie SH, Majidi Zolbanin N, Ahmadi A, Bagherifar R, Valizadeh H, Kashanchi F, *et al.* Recent
394 advances in mRNA-LNP therapeutics: immunological and pharmacological aspects. *J*
395 *Nanobiotechnology* **2022**;20:276
- 396 2. Zong Y, Lin Y, Wei T, Cheng Q. Lipid Nanoparticle (LNP) Enables mRNA Delivery for Cancer
397 Therapy. *Adv Mater* **2023**:e2303261
- 398 3. August A, Attarwala HZ, Himansu S, Kalidindi S, Lu S, Pajon R, *et al.* A phase 1 trial of lipid-
399 encapsulated mRNA encoding a monoclonal antibody with neutralizing activity against
400 Chikungunya virus. *Nat Med* **2021**;27:2224-33
- 401 4. Jiang L, Park JS, Yin L, Laureano R, Jacquinet E, Yang J, *et al.* Dual mRNA therapy restores
402 metabolic function in long-term studies in mice with propionic acidemia. *Nat Commun*
403 **2020**;11:5339
- 404 5. de Picciotto S, DeVita N, Hsiao CJ, Honan C, Tse SW, Nguyen M, *et al.* Selective activation and
405 expansion of regulatory T cells using lipid encapsulated mRNA encoding a long-acting IL-2
406 mutein. *Nat Commun* **2022**;13:3866
- 407 6. Hewitt SL, Bai A, Bailey D, Ichikawa K, Zielinski J, Karp R, *et al.* Durable anticancer immunity from
408 intratumoral administration of IL-23, IL-36gamma, and OX40L mRNAs. *Sci Transl Med* **2019**;11
- 409 7. Khattak AC, M.; Meniawy, T.; Ansstas, G.; Medina, T.; Taylor, M.H.; Kim, K.B.; McKean, M.; Long,
410 G.V.; Sullivan, R.J.; Faries, M.; Tran, T.; Cowey, C.; Pecora, A.; Segar, J.; Atkinson, V.; Gibney, G.T.;
411 Luke, K.; Thomas, S.; Buchbinder, E.; Hou, P.; Zhu, L.; Zaks, T.; Brown, M.; Aanur, P.; Meehan,
412 R.S.; Weber, J.S. A personalized cancer vaccine, mRNA-4157, combined with pembrolizumab
413 versus pembrolizumab in patients with resected high-risk melanoma; Efficacy and safety results
414 from the randomized, open-label Phase 2 mRNA-4157-P201/Keynote-942 trial. *American*
415 *Association of Cancer Research* **2023**
- 416 8. Khattak AW, J.S.; Menjawy, T.; Taylor, M.H.; Ansstas, G.; Kim, K.B.; McKean, M.; Long, G.V.;
417 Sullivan, R.J.; Farier, M.B.; Tran, T.; Cowey, C.L.; Medina, T.M.; Segar, J.M.; Atkinson, V.; Gibney,
418 G.T.; Luke, J.J.; Buchbinder, E.I.; Meehan, R.S.; Carlino, M.S. Distant metastasis-free survival
419 results from the randomized, phase 2 mRNA-4157-P201/KEYNOTE-942 trial. *American Society of*
420 *Clinical Oncology* **2023**
- 421 9. Attarwala H, Lumley M, Liang M, Ivaturi V, Senn J. Translational
422 Pharmacokinetic/Pharmacodynamic Model for mRNA-3927, an Investigational Therapeutic for
423 the Treatment of Propionic Acidemia. *Nucleic Acid Ther* **2023**;33:141-7
- 424 10. de Silva S, Fromm G, Shuptrine CW, Johannes K, Patel A, Yoo KJ, *et al.* CD40 Enhances Type I
425 Interferon Responses Downstream of CD47 Blockade, Bridging Innate and Adaptive Immunity.
426 *Cancer Immunol Res* **2020**;8:230-45
- 427 11. Yoo KJ, Johannes K, Gonzalez LE, Patel A, Shuptrine CW, Opheim Z, *et al.* LIGHT (TNFSF14)
428 Costimulation Enhances Myeloid Cell Activation and Antitumor Immunity in the Setting of PD-
429 1/PD-L1 and TIGIT Checkpoint Blockade. *J Immunol* **2022**;209:510-25
- 430 12. Lakhani NJS, D.; Richardson, D.L.; Dockery, L.E., Van Le, L.; Call, J.; Rangwala, F.; Scholl, A.; Wang,
431 G.; Ma, B.; Metenou, S.; Pandite, L.; Hamilton, E. Phase 1 dose escalation study of SL-172154
432 (SIRP α -Fc-CD40L) in platinum-resistant ovarian cancer. *American Society of Clinical Oncology*
433 **2023**
- 434 13. Shuptrine CW, Perez VM, Selitsky SR, Schreiber TH, Fromm G. Shining a LIGHT on myeloid cell
435 targeted immunotherapy. *Eur J Cancer* **2023**;187:147-60
- 436 14. Kucka K, Wajant H. Receptor Oligomerization and Its Relevance for Signaling by Receptors of the
437 Tumor Necrosis Factor Receptor Superfamily. *Front Cell Dev Biol* **2020**;8:615141

- 438 15. Fromm GdS, S.; Schreiber, T.H. Reconciling Intrinsic Properties of Activating TNF Receptors by
439 Native Ligands Versus Synthetic Agonists. *Frontiers in Immunology* **2023**
- 440 16. Croft M, Benedict CA, Ware CF. Clinical targeting of the TNF and TNFR superfamilies. *Nat Rev*
441 *Drug Discov* **2013**;12:147-68
- 442 17. Nelson J, Sorensen EW, Mintri S, Rabideau AE, Zheng W, Besin G, *et al.* Impact of mRNA
443 chemistry and manufacturing process on innate immune activation. *Sci Adv* **2020**;6:eaaz6893
- 444 18. Sabnis S, Kumarasinghe ES, Salerno T, Mihai C, Ketova T, Senn JJ, *et al.* A Novel Amino Lipid
445 Series for mRNA Delivery: Improved Endosomal Escape and Sustained Pharmacology and Safety
446 in Non-human Primates. *Mol Ther* **2018**;26:1509-19
- 447 19. Al Shoyaib A, Archie SR, Karamyan VT. Intraperitoneal Route of Drug Administration: Should it
448 Be Used in Experimental Animal Studies? *Pharm Res* **2019**;37:12
- 449 20. Kunert R, Reinhart D. Advances in recombinant antibody manufacturing. *Appl Microbiol*
450 *Biotechnol* **2016**;100:3451-61
- 451 21. Johnson MLS, L.L., Hong, D.; Schoffski, P.; Galvao, V.; Rangwala, F.; Hernandez, R.; Gonzalez, L.;
452 Ma, B.; Pandite, L.; Brana, I. Phase 1 dose escalation of an agonist redirected checkpoint (ARC)
453 fusion protein, SL-279252 (PD1-Fc-OX40L), in subjects with advanced solid tumors or
454 lymphomas (NCT03894618). *Society for the Immunotherapy of Cancer* **2022**
- 455 22. Fromm G, de Silva S, Johannes K, Patel A, Hornblower JC, Schreiber TH. Agonist redirected
456 checkpoint, PD1-Fc-OX40L, for cancer immunotherapy. *J Immunother Cancer* **2018**;6:149
- 457 23. Munter R, Christensen E, Andresen TL, Larsen JB. Studying how administration route and dose
458 regulates antibody generation against LNPs for mRNA delivery with single-particle resolution.
459 *Mol Ther Methods Clin Dev* **2023**;29:450-9
- 460 24. Pardi N, Tuyishime S, Muramatsu H, Kariko K, Mui BL, Tam YK, *et al.* Expression kinetics of
461 nucleoside-modified mRNA delivered in lipid nanoparticles to mice by various routes. *J Control*
462 *Release* **2015**;217:345-51
- 463 25. Lakhani N.J. SD, Richardson D.L., Dockery L.E., Van Lee L., Call J., Rangwala F., Scholl A., Wang G.,
464 Ma B., Metenou S., Pandite L., Hamilton E. Phase 1 dose escalation study of SL-172154 (SIRP α -
465 Fc-CD40L) in platinum-resistant ovarian cancer. *American Association of Clinical Oncology*
466 **2023**;Annual Meeting
- 467 26. Daver N. SAS, Bixby D., ChaiHo W., Zeidner J.F., Maher K., Stevens D., Stahl M., Yee K., Curran
468 E.K., Ito S., Sochacki A., Sallman D., Hernandez R., Metenou S., Ma B., Kato K., Zeidan A.M.
469 Safety, Pharmacodynamic, and Anti-Tumor Activity of SL-172154 as Monotherapy and in
470 Combination with Azacitidine (AZA) in Relapsed/Refractory (R/R) Acute Myeloid Leukemia
471 (AML) and Higher-Risk Myelodysplastic Syndromes/Neoplasms (HR-MDS) Patients (pts).
472 *American Society of Hematology* **2023**;Annual Meeting
- 473 27. Nagarsheth N, Wicha MS, Zou W. Chemokines in the cancer microenvironment and their
474 relevance in cancer immunotherapy. *Nat Rev Immunol* **2017**;17:559-72
- 475 28. Mukherjee J, Ondeck CA, Tremblay JM, Archer J, Debatis M, Foss A, *et al.* Intramuscular delivery
476 of formulated RNA encoding six linked nanobodies is highly protective for exposures to three
477 Botulinum neurotoxin serotypes. *Sci Rep* **2022**;12:11664
- 478 29. Hotz C, Wagenaar TR, Gieseke F, Bangari DS, Callahan M, Cao H, *et al.* Local delivery of mRNA-
479 encoded cytokines promotes antitumor immunity and tumor eradication across multiple
480 preclinical tumor models. *Sci Transl Med* **2021**;13:eabc7804
- 481 30. Liu X, Barrett DM, Jiang S, Fang C, Kalos M, Grupp SA, *et al.* Improved anti-leukemia activities of
482 adoptively transferred T cells expressing bispecific T-cell engager in mice. *Blood Cancer J*
483 **2016**;6:e430
- 484 31. Wu L, Wang W, Tian J, Qi C, Cai Z, Yan W, *et al.* Engineered mRNA-expressed bispecific antibody
485 prevent intestinal cancer via lipid nanoparticle delivery. *Bioengineered* **2021**;12:12383-93

487 **Figure Legends**

488 **Figure 1. Proof of concept: Can mRNA/LNP formulations encode active multimeric biologics *in vivo*?** (A)
 489 Complex, hexameric bifunctional therapies that simultaneously block an immune checkpoint (CP) or tumor
 490 associated antigen (TAA) and agonize TNF receptor/ligand (TNFR / TNFL) pathways have been successfully
 491 manufactured as fusion protein biologics and are under clinical investigation in multiple oncology trials. The
 492 mRNA/LNP generation of similar multimeric therapeutics could influence certain attributes of pharmacokinetics
 493 and pharmacodynamics, including the (B) *in vivo* production from multiple tissue compartments over an extended
 494 time-course as compared to the fusion protein exposure kinetics. (C) Fc-linked hexameric fusion proteins produced
 495 from mammalian production cell lines are secreted as monomers, that go through a stepwise process of disulfide
 496 mediated dimerization, followed by tetramer and then hexamer formation through non-covalent interactions
 497 between neighboring TNF-ligand domains. (D) The resulting hexameric fusion protein uniquely activates TNF-
 498 receptors which require trimerization for signaling. Figure generated using Biorender.

499 **Figure 2. mRNA constructs encoded functional hexameric bifunctional therapeutic fusion proteins.** (A) mRNA-
 500 encoded human SIRP α -Fc-CD40L or (B) TIGIT-Fc-LIGHT were transfected into HEK293T cells and after 48 hours, the
 501 resulting protein was affinity purified using FcXL resin. The purified protein migrated as expected in SDS-PAGE
 502 under non-reduced, BME reduced (R) and deglycosylated (DG) conditions, and was detected by three separate
 503 domain-specific antibodies. (C)(D) Per cell production of mRNA generated protein was quantitated using a dual
 504 MSD PK assay and two separate VHH reagents developed to be hexameric-fusion protein specific, for capture and
 505 detection. The mRNA generated supernatant concentrations were matched to that of fusion protein reference
 506 material (FP Ref.) and both the FP ref. and mRNA-generated protein (mRNA) were assessed head-to-head for (C)
 507 SIRP α -Fc-CD40L in (1) a dual MSD potency assay, (2) CD40 cell-based NF κ B activity assay, and (3) an *in vitro*
 508 macrophage/tumor phagocytosis assay. (D) Human *TIGIT-Fc-LIGHT* was also encoded by mRNA and characterized
 509 by western blot and a dual PK MSD assay. The resulting mRNA-generated protein concentrations were normalized
 510 to a FP ref. and assessed head-to-head in (1) a dual MSD potency assay, (2) a U2OS/NF κ B/NIK/LT β R+ cell-based
 511 reporter assay, and (3) by qPCR assessing the expression of CCL2 and CXCL8 in the LT β R+ human tumor cell line
 512 A375.

513 **Figure 3. mRNA-encoded fusion proteins were generated *in vivo* as hexameric proteins and demonstrated**
 514 **extended serum and tissue exposure kinetics.** (A) Mice were given a single dose through tail vein of 200 μ g of the
 515 FP ref., 12.5 μ g of the corresponding mRNA/LNP formulation, or vehicle. After 0.5, 1, 2, 6, 24, 48, 72, and 96
 516 hours, (B) serum, and (C) liver, spleen, and iLNs were collected from each animal (n=3 per group, per time point),
 517 and PK was assessed using MSD assay formats that captured one end of the fusion protein and detected the other.
 518 (D) Serum was collected from mRNA/LNP treated mice, pooled, and purified using a single-step ProA capture and
 519 elute method. The resulting protein was analyzed using SEC alongside of an existing human SIRP α -Fc-CD40L FP ref.
 520 control. (E) Serum cytokines were assessed in non-tumor bearing mice over the entire time-course, including the
 521 kinetic increase in IL-2 over a 96-hour period. (F) Other cytokines were more transiently increased, usually within
 522 1-2 hours of the treatment. Part A was generated using Biorender.

523 **Figure 4. mRNA-encoded fusion proteins detected in the tumor and induced on-target PD activity, anti-tumor**
 524 **response, and extended survival.** A CT26 tumor study was designed to assess the anti-tumor activity of mRNA/LNP
 525 formulated fusion proteins compared to that of the FP ref. material. Mice were inoculated on the hind flank with
 526 CT26 tumors and when the tumor volume reached ~ 90 mm³, treatment began. FP ref. were given at doses of 200
 527 μ g through IP injection, mRNA/LNPs at 12.5 μ g through IV injection, and benchmark antibodies at 100 μ g through
 528 IP injection. Treatments were given on days 0, 3, 7, 10, 14, and 17. One cohort of treated animals was assessed for
 529 tumor growth and survival over a 30-day period, and another cohort of animals was euthanized on day 8 of the
 530 time-course, 24 hours after the day 7 dose, to assess (A) therapeutic protein concentrations within the tumor and

531 (B) average serum and tumor cytokines for treated animals. (C) Individual tumor growth curves are shown for
532 each treatment group. In addition, the average day in which all animals within a treatment group reached tumor
533 burden is quantitated and shown within each graph, and also depicted as a vertical dotted line. The number of
534 animals in each group and any animals that completely rejected the established tumor are also shown within the
535 graphs. For example, the vehicle treated group reached tumor burden at an average of 13.13 days, 8 animals were
536 in this group, and 0/8 rejected the tumor. (D) The Kaplan-Meier graph depicts group survival over the time-course
537 and the Mantel-Cox test was used to assess group significance. (E) A cohort of animals was euthanized on day 8,
538 24 hours after the third dose on day 7. Tumors were excised, dissociated, and the immune infiltrate was assessed
539 by flow cytometry. Truncated violin plots depict the median, first, and third quartiles. (F) Combination efficacy of
540 FP and mRNA therapeutics was assessed with anti-PDL1 (clone 10F.9G2), which was delivered at doses of 200 µg
541 alone or in the combinations shown on days 0, 3, 7, 10, and 14. Tumor growth inhibition on day 15 of the time
542 course is shown in comparison to the vehicle control group and significance between groups was calculated using
543 unpaired t-test. (G) A cohort of treated animals from the combination study was euthanized on day 8, 24 hours
544 after the third dose on day 7. Tumors were excised, dissociated, and the immune infiltrate was assessed by flow
545 cytometry. Cell populations were normalized to those of the anti-PDL1 monotherapy (set at a value of 1) group to
546 visualize the contribution of each combination.

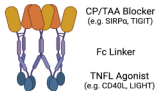
547

548

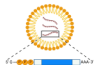
A.

Evaluation of Complex Biologics Delivered as:

(1) Multimeric Fusion Protein



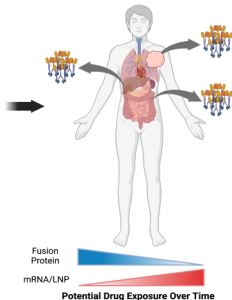
(2) mRNA/LNP Formulation



Can mRNA/LNPs generate functional oligomeric proteins *in vivo*?

B.

In Vivo Production of mRNA Encoded Protein



C.

1.



Secretion of Monomer

2.



Dimerization

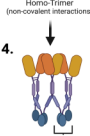
Disulfide Bonds

3.



Two Dimers Form Tetramer

4.

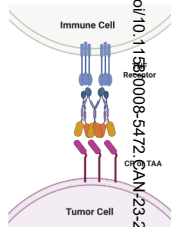


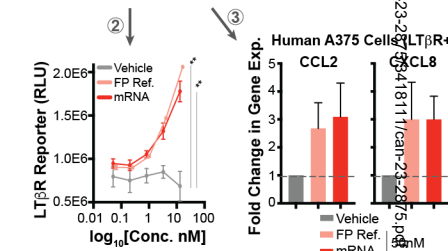
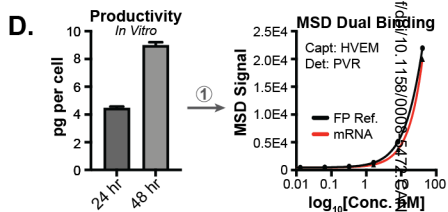
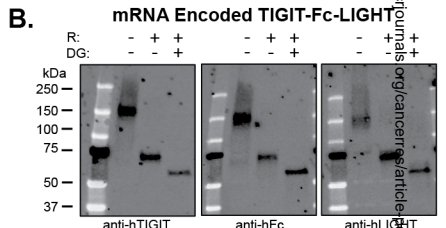
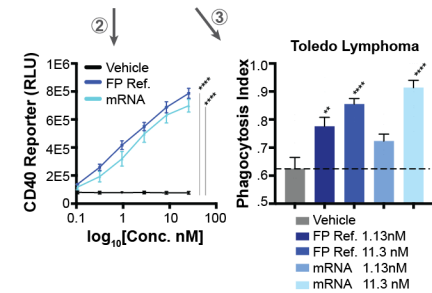
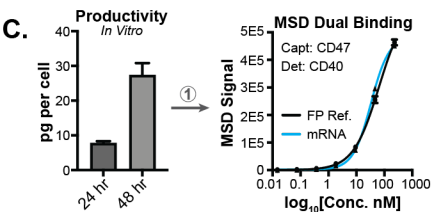
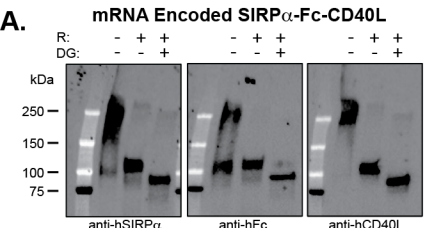
Tetramer and Free Dimer Form Hexamer

Third Dimer Completes the Second Trimer

D.

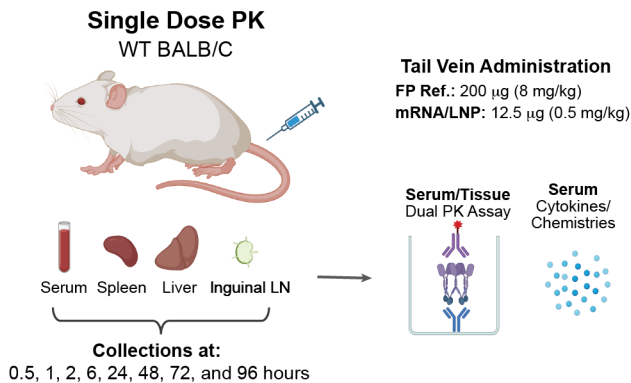
Combined Checkpoint Blockade / Immune Agonism



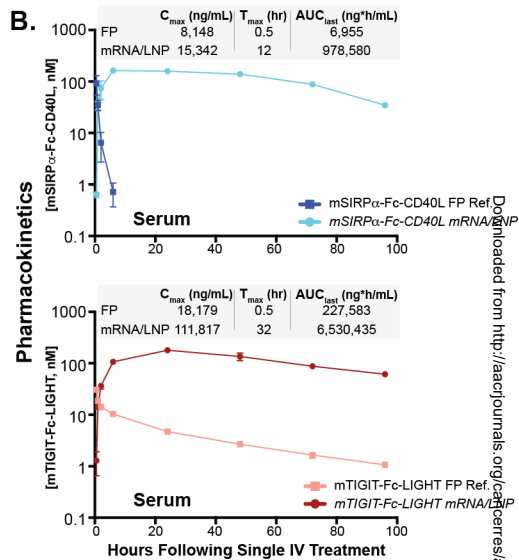


bioRxiv preprint doi: <https://doi.org/10.1101/000554>; this version posted May 23, 2015. The copyright holder for this preprint (which was not certified by peer review) is the author/funder, who has granted bioRxiv a license to display the preprint in perpetuity. It is made available under aCC-BY 4.0 International license.

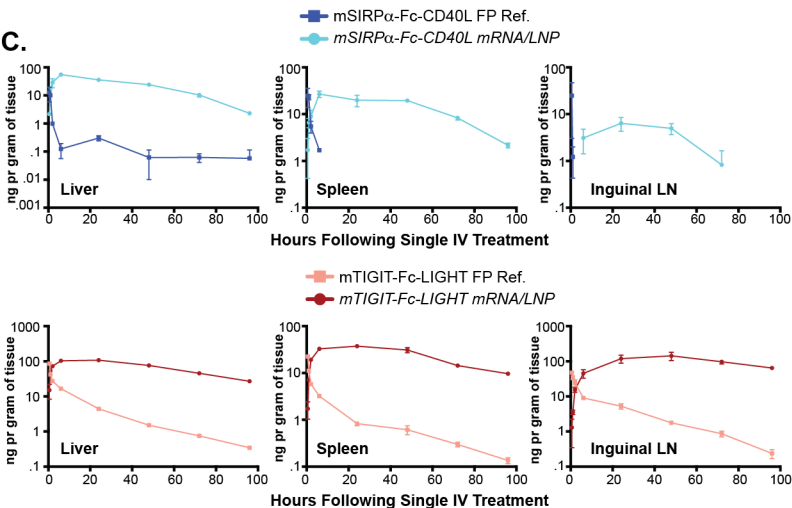
A.



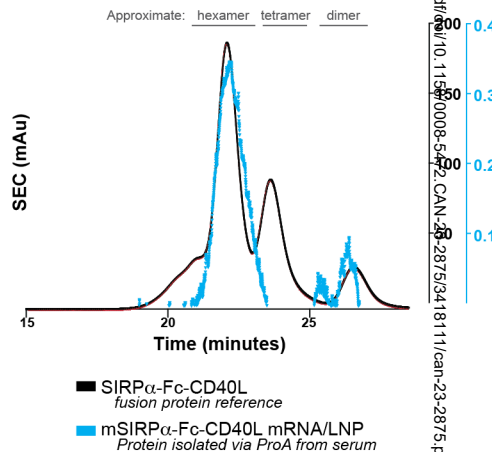
B.



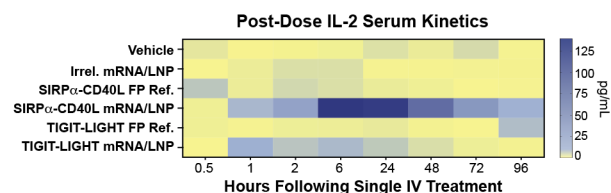
C.



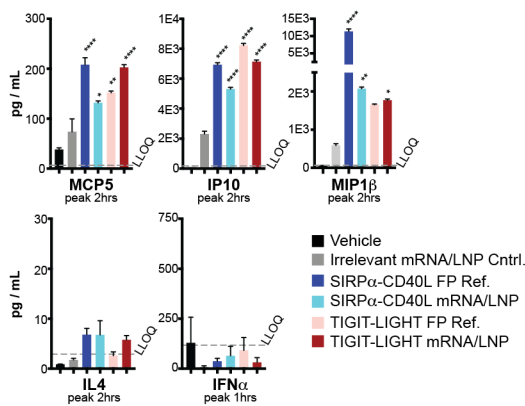
D.



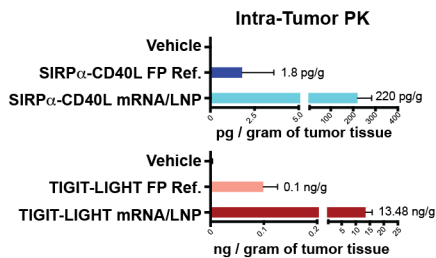
E.



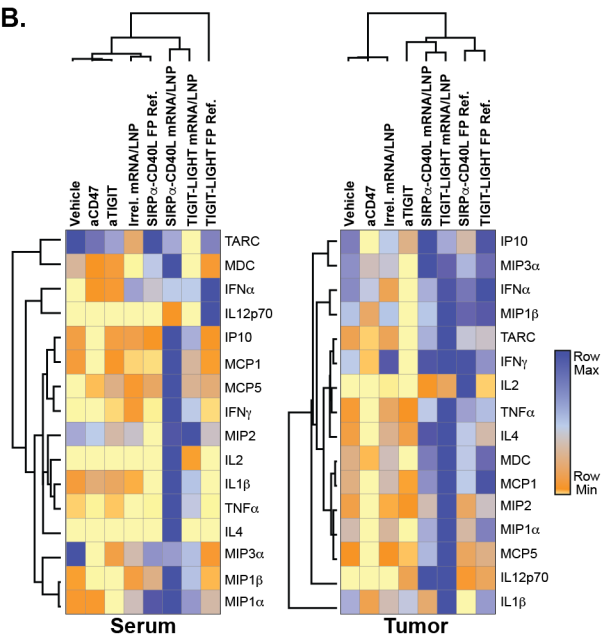
F.



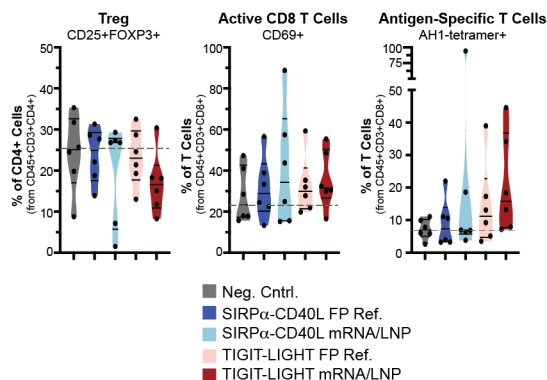
A.



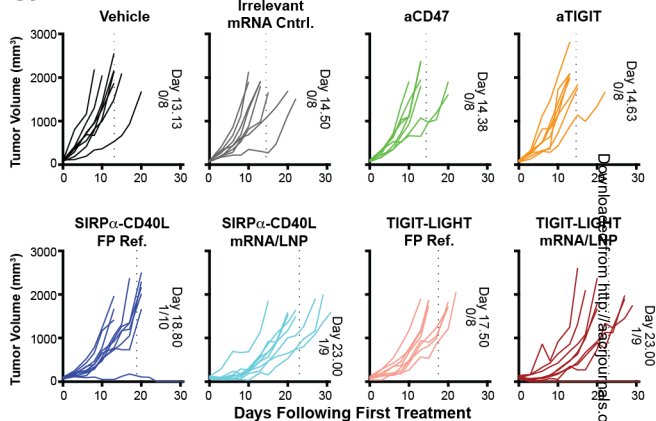
B.



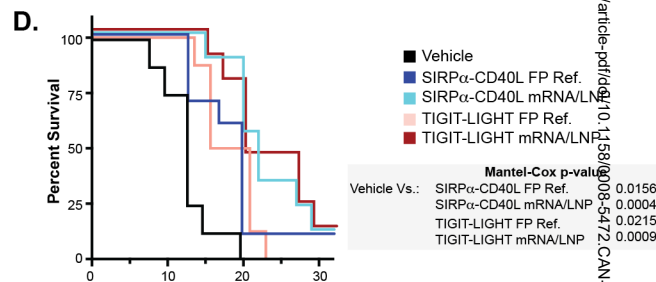
E.



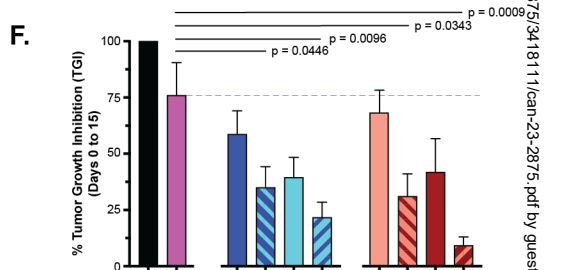
C.



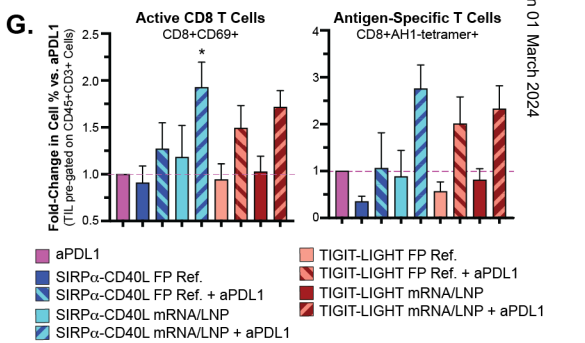
D.



F.



G.



bioRxiv preprint doi: <https://doi.org/10.1101/2023.03.14.530472>; this version posted March 23, 2024. The copyright holder for this preprint (which was not certified by peer review) is the author/funder, who has granted bioRxiv a license to display the preprint in perpetuity. It is made available under aCC-BY-NC-ND 4.0 International license.